



HAL
open science

Heterogeneous behavior modeling of a LiFePO₄-graphite cell using an equivalent electrical circuit

Nicolas Damay, Christophe Forgez, Guy Friedrich, Marie-Pierre Bichat

► To cite this version:

Nicolas Damay, Christophe Forgez, Guy Friedrich, Marie-Pierre Bichat. Heterogeneous behavior modeling of a LiFePO₄-graphite cell using an equivalent electrical circuit. *Journal of Energy Storage*, 2017, 12, pp.167 - 177. 10.1016/j.est.2017.04.014 . hal-01522589

HAL Id: hal-01522589

<https://hal.science/hal-01522589>

Submitted on 15 May 2017

HAL is a multi-disciplinary open access archive for the deposit and dissemination of scientific research documents, whether they are published or not. The documents may come from teaching and research institutions in France or abroad, or from public or private research centers.

L'archive ouverte pluridisciplinaire **HAL**, est destinée au dépôt et à la diffusion de documents scientifiques de niveau recherche, publiés ou non, émanant des établissements d'enseignement et de recherche français ou étrangers, des laboratoires publics ou privés.

Heterogeneous behavior modeling of a LiFePO₄-graphite cell using an equivalent electrical circuit

Nicolas Damay^a, Christophe Forgez^{a,*}, Guy Friedrich^a, Marie-Pierre Bichat^b

^a*Sorbonne universités, Université de technologie de Compiègne
Laboratoire d'Electromécanique de Compiègne, EA 1006
Centre de recherche Royallieu, CS 60319, 60203 Compiègne cedex (France)*
^b*E4V, 9 avenue Georges Auric, 72000 Le Mans (France)*

Abstract

The increasing demand for cost-effective and high-performance batteries makes accurate models essential to improve and control them over their entire life time. Recent studies have pointed out that the heterogeneity of a cell electrical behavior plays an important role in its overall performances. In this paper, an equivalent electrical circuit is built thanks to a physical approach to model the heterogeneous behavior of a commercial LiFePO₄-graphite cell. Unlike classical homogeneous models, the parameters of this “multibunch model” do not require to be functions of the state of charge (SoC) to bring accurate results. The equivalent electrical parameters are assumed to follow a distribution law and the latter is determined experimentally for the studied cell. The multibunch model is able to reproduce many features of a cell electrical dynamic: disappearance of the open-circuit voltage (OCV) shape at high current, performances decrease, longer relaxation time, electrical losses during relaxation and high local stress. Thanks to the removal of the parameters dependencies to SoC, the duration of the electrical parameters measurements on the whole operating-range of the battery can be shortened. We estimate that it can be reduced from more than 30 days to about 3 days. Moreover, the determination of the internal resistance distribution could be the basis of a non-invasive tool to characterize the quality of a cell or electrode during its entire lifespan.]

Keywords: Batteries, Electrical Modeling, Heterogeneity, Parameter Distribution, Non-Linearity.

1. Introduction

Energy production and management is one of the key challenges of our societies and energy storage devices have a central role in it. All battery users (electronic devices, electric transportation, grid services) are concerned with the safety, cost, autonomy and reliability of their batteries [1]. Researchers are addressing these issues in many different ways. New electrode materials are being developed [2]. Methods to improve the battery conception and management are proposed [3, 4, 5, 6]. The possibility to re-use traction batteries for grid services is explored, because it is a good opportunity to make them more cost-attractive and to meet the energy-storage devices demand due to the rise of renewable energies [2, 7].

Enhanced models are still needed in order to understand performance limiting mechanisms, to improve batteries integration in commercial products or to create non-invasive diagnostic tools to track their state of health. This study is focused on one particular factor that has a strong impact on the battery performances, namely the heterogeneity of their electrical behaviors.

Experimental studies have been led on specially designed cells in order to characterize their heterogeneity. Ouvrard *et al.* [8] studied a LiFePO₄ electrode and they observed a heterogeneous behavior during high current rate operation. They discovered that a non-uniform pressure significantly affects the heterogeneity, suggesting an important contribution of the electrical connection between active material particles. Osswald *et al.* [9] manufactured a LiFePO₄-graphite cell that allows local potentials measurements during operation. They demonstrated that transitions between the OCV plateaus are reached at different times, depending on the current rate, and that some parts of the cell can be depleted before the others, leading to a decrease of the available capacity. Zhang *et al.* [10] also proved experimentally that the usable energy of a LiFePO₄-graphite cell is reduced if the current distribution is non-uniform during operation. They observed high local stresses due to small local resistivity, which are likely to locally damage the active materials.

From this overview of the literature, it is clear that the heterogeneity has a strong influence at the cell level and it should be taken into account in an enhanced electrical model to further improve its capabilities.

PDE (partial differential equations) models can be very

*Corresponding author

Email address: christophe.forgez@utc.fr (Christophe Forgez)

accurate because they can take into account every physical phenomena occurring within a cell, making them interesting to spot and to understand the performance-limiting factors [11, 12, 13, 14]. Bernardi and Go [15] demonstrated through a PDE model that during high current pulse, the SoC (State of Charge) drift at particles surfaces can be three times larger than the cell mean SoC, leading to higher local fatigue. Farkhondeh *et al.* [16] used a PDE model to reproduce measured constant rate discharges. They managed to significantly improve the model response by considering several active material particles with different sizes and different electronic connectivities to the solid matrix, proving the benefit of taking heterogeneity into account.

Though PDE models are powerful tools, their numerous parameters are difficult to obtain. Another approach is to only model the main electrochemical phenomena to build an equivalent circuit model (ECM) [17]. The well-known Randles model, whose construction is recalled in section 2, is also based on a physical approach, but its parameters are easier to extract at the user-level [18, 19, 20].

Unfortunately, the determination of a Randles model parameters may require weeks of tests to cover a battery whole operating range, because these parameters are highly non-linear regarding the current, temperature and SoC [21, 22, 23]. Besides, representing both polarization and relaxation dynamics requires the use of two different models or the use of two different sets of electrical parameters [5, 24].

One major assumption of the Randles model is to consider a battery as a homogeneous system. In this study, we propose an ECM called “Multibunch Model” that takes into account the heterogeneous electrical-behavior of a cell. We demonstrate that the proposed model is able to accurately reproduce most of a cell electrical-dynamic features without introducing any SoC non-linearities of its parameters, excepting for the OCV (Open-Circuit Voltage).

Before presenting the multibunch model, some limitations of the homogeneous Randles model are illustrated in the section 2. Section 3 is dedicated to the construction of the proposed model based on a physical approach. Then, the electrical-dynamic features (called “heterogeneity signatures”) due to internal heterogeneity are detailed and discussed in a fourth part and their changes due to the model parameters distribution-shape are highlighted in section 5. Finally, the equivalent internal resistance distribution of a commercial LiFePO₄-graphite cell is determined and implemented in the multibunch model to experimentally validate its capability.

2. Homogeneous models limitations

After presenting the classical Randles model, some of its limitations are presented in this section. More specifically, the SoC-dependency of its parameters is presented and their necessity is illustrated by comparing a simulation to measurements.

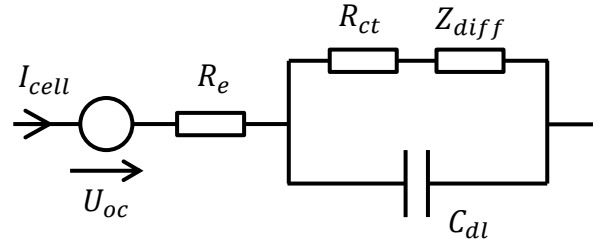


Figure 1: The Randles model, which is a classical homogeneous equivalent electrical circuit for an electrochemical cell.

2.1. Randles model presentation

The Randles model, presented in figure 1, is composed of several elements that represent the main electrochemical phenomena occurring during a cell operation [17]:

- a voltage source U_{oc} stands for the OCV ;
- a resistance R_e represents the resistive contributions of the electrolyte and current collectors;
- a resistance R_{ct} models the charge transfer between the electrolyte and the active materials;
- a capacitance C_{dl} accounts for the double layer effect that occurs at the interface between the electrolyte and the active materials;
- an equivalent diffusion impedance Z_{diff} that reproduces the apparent behavior of the charges diffusion-phenomenon within the active materials.

This model has been used in a previous study to explain how to combine it with a thermal model and how its parameters are determined [25]. The study has been made on a commercial 40Ah LiFePO₄-graphite prismatic cell (maximum continuous discharge rate of 3C). It has been stated that the electrical parameters are strongly dependent on the cell temperature, current and SoC. More specifically, the SoC dependency of this cell quasi steady-state resistance R_{QS} , which corresponds to the sum of all resistive contributions in the cell, has been represented in figure 2 for 1C charge and discharge at 45°C.

R_{QS} evolves significantly with the SoC, its major rises being near SoC 100% during charge and near SoC 0% during discharge. Some variations of the R_{QS} resistance can be observed around SoC 15%, 45 % and 80%. They are due to the OCV curve variations (figure 3), that lead to changes in the apparent resistance of the cell. This feature is discussed in section 4.4.

The OCV curves in the figure 3 are actually the envelopes of all possible values of the OCV. In this study, the hysteretic behavior of U_{oc} has been modeled by (Equation 1) [24].

$$U_{oc}(SoC, h) = U_{oc,Ch}(SoC) \times h + U_{oc,Dch}(SoC) \times (1 - h) \quad (1)$$

$U_{oc,Ch}$ (resp. $U_{oc,Dch}$) is the upper (resp. lower) envelope of the figure 3. The hysteresis parameter h is determined thanks to an integrator defined by Equation (2). I_{cell} is the cell current, C_{cell} its faradic capacity and m a parameter defining how many SoC percent are needed for h to go from 0 to 1. In this study, the latter has been set to 15% [24].

$$h(t) = \int \frac{m \times I_{cell}}{C_{cell}} dt \quad \text{with } h(t) \in [0, 1] \quad (2)$$

The hysteresis parameter h is limited by two saturation values, namely 0 and 1. That is to say, if the result of Equation (2) should exceed 1 (resp. go below 0), the value of h remains 1 (resp. 0).

2.2. Illustration of the SoC non-linearities need in a homogeneous ECM

The homogeneous Randles model being presented, the following subsection is focused on its parameters non-linearities regarding SoC. In order to highlight their importance, a simulation has been made while neglecting them. The

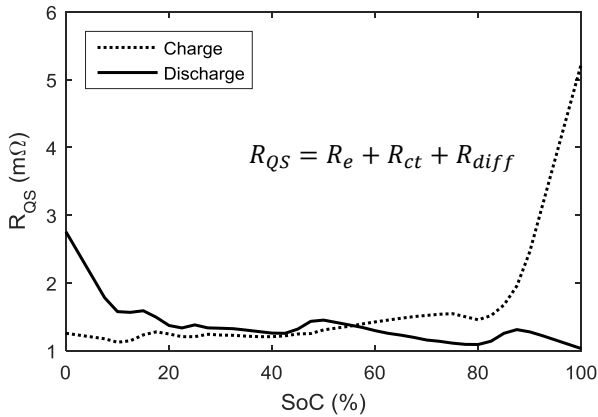


Figure 2: SoC dependency of the quasi steady-state resistance of a commercial 40Ah LiFePO₄-graphite cell for 1C charge and discharge at 45°C. [26].

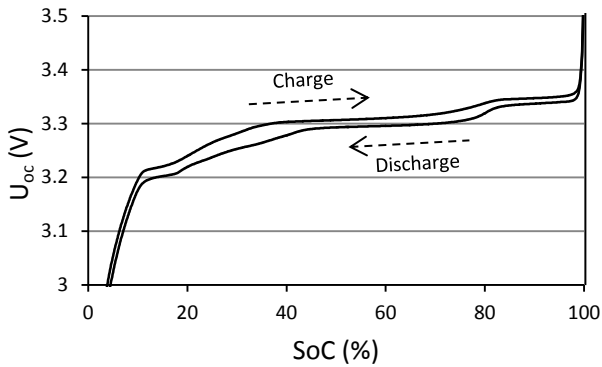


Figure 3: OCV curves of the studied cell in charge and discharge as functions of the SoC. [26].

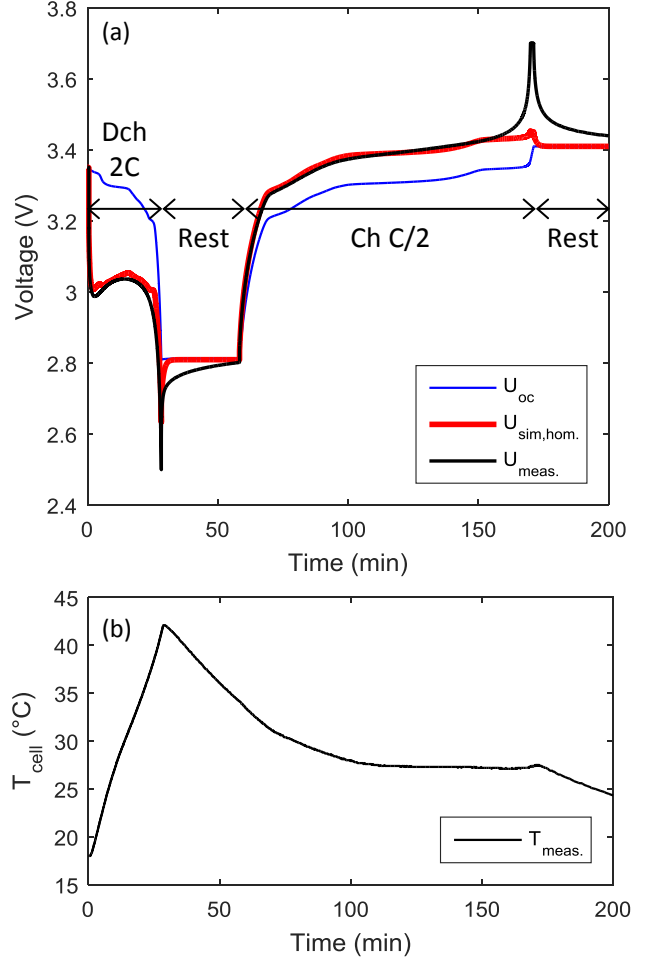


Figure 4: Measurements on the studied cell during a validation test [25]. (a) Measured cell voltage with OCV estimation and a homogeneous model prediction with parameters depending on current and temperature, but constant regarding SoC. (b) Surface temperature measurements.

electrical model has been used to reproduce the cell voltage measured during a specific test, with its parameters depending only on current and temperature (their values have been considered at SoC 50%).

The reference test of this study has been realized on the same commercial 40Ah LiFePO₄-graphite cell as in a previous work [25]. Its bottom face was placed on a support regulated at 15 °C and its other faces and power wires were wrapped with insulating materials. It has been fully discharged at 2C rate, then kept in open-circuit for 30 min, fully charged at C/2 rate and kept in open-circuit for 30 min again. The temperature and voltage measurements are represented in figure 4. The OCV of the cell has been estimated and reported in the figure, along with the simulated voltage.

The voltage relaxation during rest periods is badly modeled: the voltage returns to the OCV value too quickly because the diffusion-dynamic determined for the polarization is also used for the relaxation. The simulation is close to the measurements during most of the charge, but there

is a strong discrepancy at its end. During the 2C discharge, the voltage is over-estimated and, because it follows the OCV shape, it is “bumpy” compared to the measurement. The error at the end of the discharge reaches 134 mV. Apart from the relaxation dynamic, these inaccuracies can be improved by making the electrical parameters values SoC-dependent.

In order to avoid the use of such SoC non-linearities, we propose a new ECM which takes into account the heterogeneity of the cell electrical behavior. It is presented in the following section.

3. Multibunch model construction

An electrochemical cell can be pictured as numerous elementary parts assembled together. These elements are small active-materials parts whose electrochemical properties (potential, concentration, conductivity) can be considered to be homogeneous [16].

From one elementary part to another, there is a lot of reasons for their electrochemical properties to be different: manufacturing non uniformities [27, 28], distance to the current collectors and concentration gradients within particles [15], position of the tabs within the cell [10], non-uniform pressure on the electrodes [8], local tortuosity [29], temperature gradients [30], different particles sizes [31], etc. All these differences are bound to affect the current flowing within each part, thus making the electrode operating in a heterogeneous way.

3.1. From heterogeneous electrodes to bunches construction

Modeling each and every elementary part would be inefficient. Because they are numerous, it can be reasonably assumed that some of them have very close electrical properties from the tab point of view. These parts are bound to have the same electrical behavior and we propose to regroup them into homogeneous sets with equivalent electrical properties. These sets are called “bunches” and they are constructed in such a way they have the same faradic capacities.

In order to characterize the bunches electrical properties in a practical manner, they are described by a distribution function in this study. Though the use of a normal distribution to represent a random variable is classical, it appears that the distributions of battery properties such as resistances, capacities or even particle sizes can be right- or left-skewed [16, 27, 31]. Schuster *et al.* [27] have proposed to use a 3-parameter Weibull distribution, because it is more versatile. Moreover, its outputs are positive values, which is physically necessary for describing these properties.

A 3-parameter Weibull distribution is defined by Equation (3) with θ as a location parameter, λ as a scale parameter and k as a shape parameter. A shape coefficient of 3.5 lead to a symmetrical distribution (see section 5).

For $k < 3.5$ (resp. $k > 3.5$) the distribution is left-skewed (resp. right-skewed).

$$f(x) = \frac{k}{\lambda} \left(\frac{x - \theta}{\lambda} \right)^{k-1} \exp^{-\left(\frac{x-\theta}{\lambda}\right)^k} \quad \text{with } x > 0 \quad (3)$$

3.2. Bunches modeling by simplified Randles circuits

The electrical behavior of each bunch is modeled by a homogeneous Randles model. The multibunch model is then obtained by connecting all the bunches models in parallel, the cell voltage U_{cell} being found at the terminals of the bunches (Figure 5).

The double layer capacities (section 2.1) have been neglected to reduce the computational time. Therefore, the bunches models contain “high-frequency resistances” $R_{HF,i}$ (with $i \in [1, 2, \dots, n]$) which represent the voltage drop due to the electrolyte and to the charge transfer resistances. A single RC circuit stands for the diffusive phenomenon. This approximation of the limited diffusion behavior significantly reduce computational time and it is considered to be sufficient to illustrate the conclusions of this study [25].

An important component for each bunch is the voltage source $U_{th,i}$, which represents its thermodynamic equilibrium voltage (TEV). It is similar to the homogeneous model OCV curve, but because a bunch cannot be in open-circuit, it would be inaccurate to use the “OCV” term. Its value depends on the state of charge SoC_i of the corresponding bunch, in accordance with the curve reproduced in figure 3. It has an hysteretic behavior which depends on the corresponding bunch current. The particular contributions of these bunches TEV to the cell electrical dynamic is discussed in section 4.2.

According to the literature, each parameter of the proposed model should be distributed because the corresponding physical parameters are bound to be distributed. The high frequency resistances $R_{HF,i}$ are related to the contact resistances, to the electronic-paths lengths between a tab and a given particle, to the pressure applied on the electrode and eventually to its local tortuosity. The diffusion resistances $R_{diff,i}$, as well as the diffusion time constants $\tau_{diff,i}$ ($= R_{diff,i} \times C_{diff,i}$), are linked with particles sizes *via* diffusion lengths [32].

More information can be found in the literature about the main contributions to heterogeneity. Zhang *et al.* [33] proved through measurement that the current distribution within a cell is less dispersed at high temperature than at low temperature, suggesting an important participation of the charge transfer resistance to heterogeneity. Moreover, Ouvrard *et al.* [8] observed that the heterogeneous behavior depended on the local pressure applied to a LiFePO₄ electrode. They inferred that this pressure has an effect on the contact resistances between particles or between particles and the current collector. As a result, these resistances dispersion would be important compared to other contributions. We hence simplified our model by applying

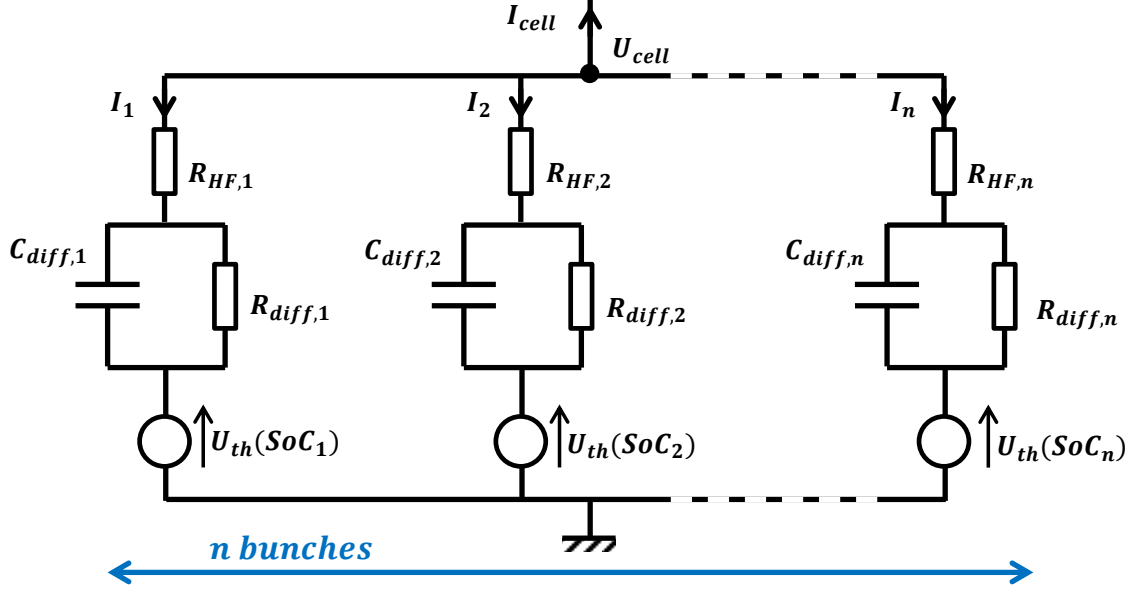


Figure 5: Multibunch model of a cell, which is divided into n bunches with different electrical properties and connected in parallel.

a distribution only on the $R_{HF,i}$. The diffusion parameters $R_{diff,i}$ and $C_{diff,i}$ are assumed to be the same for each bunch.

To compute each $R_{HF,i}$ values according to the Weibull distribution (Equation (3)), only the shape parameter k and a RSTD (Relative Standard Deviation) value are set. The values of the scale and localization parameters λ and θ are then obtained thanks to an optimization algorithm. The objective of the optimization is to make the equivalent resistance of the bunches-resistances in parallel equal to the corresponding measured resistance at SoC 50% (as measured for a homogeneous model [25]).

3.3. Current and temperature dependencies of the electrical parameters

As for a homogeneous model, the multibunch model parameters depend on current and temperature. These dependencies are based on lookup-tables obtained through experimental measurements [25]. In this study, the cell is assumed to be isothermal and any parameter variation due to thermal gradients is hence neglected.

In order to adapt the look-up tables to the distributed $R_{HF,i}$, the latter values are first determined at 1C (-40 A), 25 °C, in accordance with the above explanation. Then, their evolution regarding current and temperature are computed thanks to a coefficient $\beta(I, T)$ calculated from the parameters tables (Equation (4)). The use of this coefficient does not change the distribution shape or RSTD, making it consistent with the use of distributed parameters.

$$\begin{aligned} R_{HF,i}(I, T) &= R_{HF,i}(1C, 25^\circ C) \times \beta(I, T) \\ \beta(I, T) &= R_{HF,mes}(I, T) \div R_{HF,mes}(1C, 25^\circ C) \end{aligned} \quad (4)$$

The other parameters, namely $R_{diff,i}$ and $C_{diff,i}$ are assumed to be the same for each bunch. The diffusion resistances $R_{diff,i}$ values correspond to an extensive physical property and are thus calculated by multiplying the measured value of R_{diff} at 50% SoC by the number of bunches n (Equation (5)). $C_{diff,i}$ are calculated in such a way the diffusion time constant τ_{diff} remains the same as in the homogeneous case.

$$\begin{aligned} R_{diff,i}(I, T) &= n \times R_{diff,mes}(I, T, 50\%SoC) \\ C_{diff,i}(I, T) &= \tau_{diff,mes}(I, T) \div R_{diff,i}(I, T) \end{aligned} \quad (5)$$

3.4. Synthesis of the models hypothesis

In order to summarize the differences between the homogeneous and heterogeneous models, their main features have been reported in Tables 1 and 2. In particular, the models parameters dependencies to SoC, current I and temperature T are reported. The latter are computed thanks to 1D, 2D or 3D lookup-tables (LUT), the only exception being the hysteretic behavior of the OCV.

	Dependencies		
	SoC	T	I
U_{oc}	LUT (1D)	\emptyset	Hyst.
R_e	LUT (3D)		
R_{ct}	LUT (3D)		
C_{dl}	LUT (3D)		
Z_{diff}	LUT (3D)		

Table 1: Summary of the presented homogeneous model features

The reduction of the LUT from 3D to 2D is one of the main benefits of the multibunch model. This is useful

	Dependencies			Distrib.
	SoC	T	I	
$U_{th,i}$	LUT (1D)	\emptyset	Hyst.	\emptyset
$R_{HF,i}$ ($R_{e,i} + R_{ct,i}$)	\emptyset	LUT (2D)		Weibull
$R_{diff,i}$	\emptyset	LUT (2D)		\emptyset
$\tau_{diff,i}$	\emptyset	LUT (2D)		\emptyset

Table 2: Summary of the proposed heterogeneous model features

to speed up the characterization process of a cell and to reduce the impact of measurements errors.

Although the cell has been discretized into small elements, the proposed model is zero-dimensional, because the bunches are not associated to specific locations (as it would be the case with transmission line models [34]). The core idea is to represent how fast different parts of a single cell are charged/discharged compared to each other and how they interact.

In sections 4 and 5, the effects of heterogeneity on a cell behavior are described thanks to several simulations. In particular, it is demonstrated that the whole cell overvoltage appears to be SoC-dependent whereas the model parameters are constant regarding SoC (apart from the bunches TEV).

4. Electrical-dynamic features due to heterogeneity

This section is dedicated to the effects of heterogeneity on a LiFePO_4 -graphite cell behavior. These “heterogeneity signatures” are detailed and discussed through several examples in order to highlight the inner functioning of the model. To begin with, the simulations of charges and discharges at different constant current rates are presented in Figure 6. The parameters values are considered at 25 °C. The distribution of the $R_{HF,i}$ is based on a Weibull distribution with a shape parameter k of 2.5 and an RSTD of 40 % (cf. section 3).

4.1. Disappearance of the OCV shape

The simulated OCV curves in charge and discharge have been added to figure 6 to get a better understanding of the simulation results. Charge and discharge voltages at C/10 are close in shape to the OCV curves with only a light “smoothing”. This feature becomes more and more pronounced as the current rate is increased. During the discharges at higher rates, only the first transition between the two OCV plateaus can be distinguished. At the ends of the discharges above C/2, the OCV shape has totally vanished and the overvoltage is larger. As a consequence, the voltage limit at 2.6 V is reached sooner.

The same observations can be made for the charges: they all have the same shapes until 30% SoC. Then, the transition between the two OCV plateaus disappears and the voltage limit is reached sooner at higher current rates,

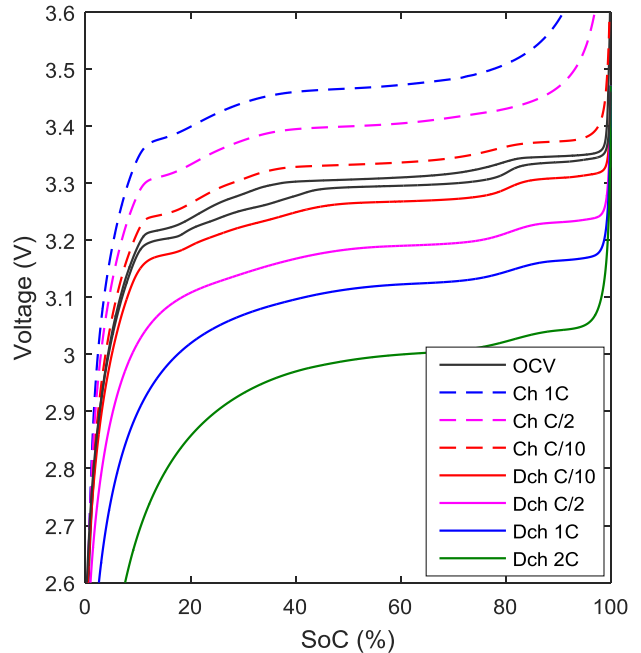


Figure 6: Simulations of full charges and discharges of a cell at different current rates and OCV curves.

thus decreasing the available capacity. It can be noticed that whereas the OCV is nearly a right-angled corner at the end of the charge, the voltage response is more and more round when the current is increased.

The first simulation results presented in figure 6 are very similar to typical charging and discharging curves of a LiFePO_4 -graphite cell and the evolution of the apparent resistance is in accordance with the R_{QS} evolution of figure 2. In order to understand the underlying functioning of the modeled heterogeneous behavior, the 2C discharge case has been reported in figure 7a with more details.

The simulated OCV curve based on the mean SoC of the cell has been kept (black curve), along with the cell voltage (red curve). The bunches resistances distribution is reported in the lower right corner. The voltage response obtained in the homogeneous case (using one bunch) has been added (blue dotted curve). Besides, the $U_{th,i}$ of each bunch have been represented (thin colored lines) to help the reader tracking the bunches states of charge SoC_i evolutions.

The differences between the homogeneous and heterogeneous voltage responses appear clearly on figure 7a. The homogeneous response has the same shape as the OCV whereas it is very smoothed in the heterogeneous case. In the latter, this is because the typical transitions of the OCV curve are not reached at the same times by the bunches. For instance, the transition between the OCV plateaus that occurs at 6 min in the homogeneous case is spread between 3 and 9 min in the heterogeneous case. Consequently, this transition is less apparent on the cell voltage.

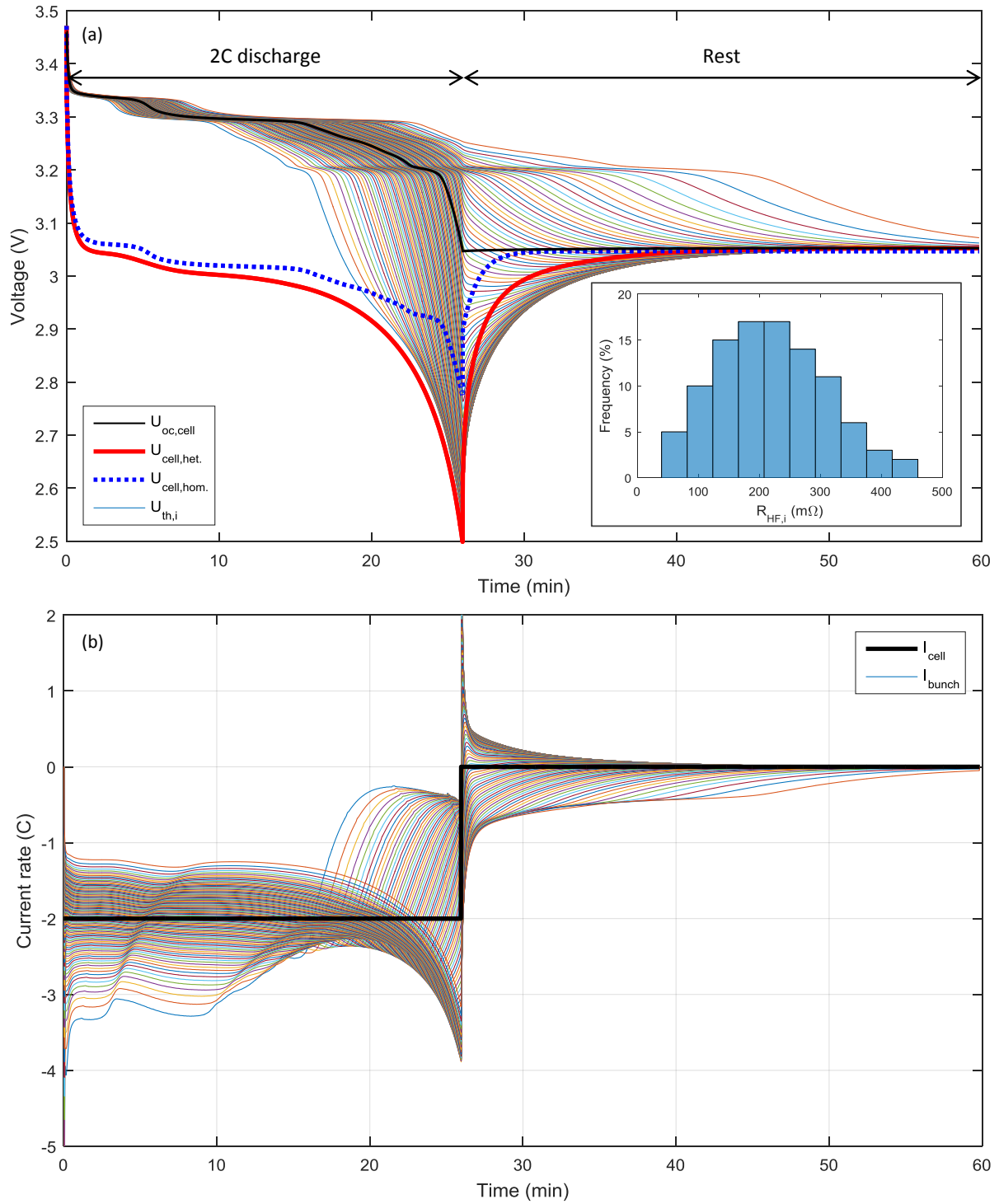


Figure 7: Simulation of the 2C discharge of a single cell followed by a rest period in open-circuit. (a) Voltage response of the multibunch model with 100 bunches (heterogeneous case) and with 1 bunch (homogeneous case) using a Weibull distribution on the $R_{HF,i}$ resistances (shape coefficient $k = 2.5$ and a RSTD of 40%). The local TEV are represented as thin lines. (b) Cell current profile and currents flowing through the bunches (expressed in C-rate).

Assuming this heterogeneous model is representative of a real-cell behavior, we point out that the use of an OCV curve related to the cell mean SoC can lead to some inaccurate interpretations concerning the cell overvoltage, with direct consequences on the determination of an equivalent resistance or for electrical losses estimation (cf. subsection 4.4).

4.2. Performances decrease

The performances of the cell during the 2C discharge, in terms of available capacity and available power, are decreased because the overvoltage is significantly increased while approaching 0% SoC. This feature due to heterogeneity is complex to describe because there is a strong coupling between the bunches TEV, governing the bunches overvoltages, and the current that flows through them.

To understand this behavior, the first observation to be made is that all the bunches have nearly the same overvoltage at the beginning due to their close $U_{th,i}$. Consequently, the relative currents flowing through them depends mainly on the $R_{HF,i}$ and the less resistive bunches are discharged at the highest rates (figure 7b).

The bunch with the lowest resistance (thin blue line) is discharged at 3C until its TEV starts to fall (after 10 min), leading its current to decrease quickly. Though more and more bunches become deeply discharged, the total current flowing through the cell has to remain constant. Consequently, the other bunches currents increase gradually, along with their overvoltages. This complex mechanism leads to the gradual increase of the cell-overvoltage, as observed in figures 2 and 4.

In the case of a low current rate (like the C/10 simulation in figure 6), the bunches with the lowest resistances cannot be completely depleted before the others because their overvoltage is greatly decreased after their TEV reached a transition. Consequently, they have to “wait” for the others to reach the blocking transition before they can be used again, thus limiting the bunches SoC dispersion.

4.3. Longer relaxation times

Another feature due to heterogeneity can be observed in figure 7a after the current has been cut: the relaxation time is much longer than the one in the homogeneous case. With a homogeneous model, the voltage relaxation to the OCV correspond to the discharge of the sole RC circuit representing the diffusion (figure 1). In the heterogeneous case, all bunches have different SoC when the current is cut and balancing currents appear in open-circuit [15].

High charging currents can be observed in figure 7b for the bunches with the lowest SoC, exceeding 2C for less than one minute. Thereafter, the bunches carry on balancing significantly for about 30 min and reach an OCV value of 3.135 V. This corresponds to a cell SoC of 8 %, meaning that there is still some usable capacity within the cell. This relaxation time would be further increased if

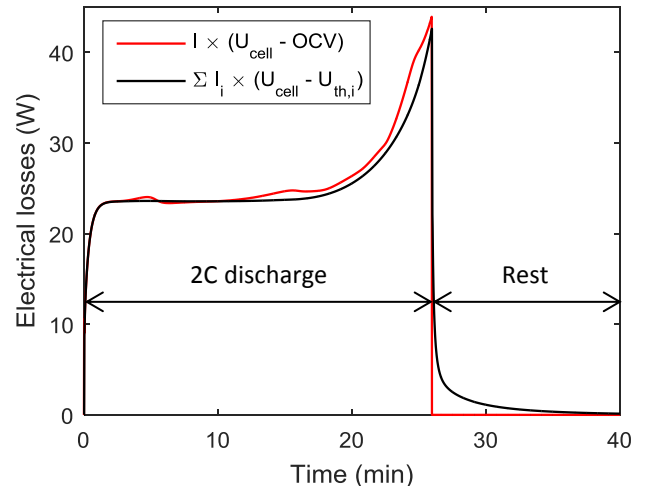


Figure 8: Simulation of the 2C discharge of a single cell followed by a rest period in open-circuit: electrical losses calculated by comparing the cell voltage and its OCV (red curve) and by summing the electrical losses of each bunch (black curve). (For interpretation of the references to color in the figure legend, the reader is referred to the web version of this article.)

the electrical parameters non-linearities regarding current had been characterized more thoroughly for small current rates, because the diffusion and charge transfer resistances tend to rapidly increase when the current decreases [35].

4.4. Electrical losses during relaxation

There is an interesting effect of heterogeneity on the electrical losses, especially during relaxation in open-circuit. Classically, the latter are calculated using Equation (6) [25] and by estimating the OCV U_{oc} thanks to the cell mean SoC (figure 3). With the multibunch model, more information about the local overvoltage and currents are available, meaning the electrical losses calculus can also be made by summing all the bunches contributions (Equation (7)).

$$\dot{Q}_{elec} = I_{cell} \times (U_{cell} - U_{oc}) \quad (6)$$

$$\dot{Q}_{elec} = \sum_{i=1}^n I_i \times (U_{cell} - U_{th,i}) \quad (7)$$

The electrical losses calculated thanks to these equations have been reported in figure 8, with the classical approach in red and the sum of bunches contributions in black. The values obtained by Equation (6) correspond to an “apparent resistance” while the results obtained by summing the bunches contributions (Equation (7)) should be more representative of the real electrical losses.

Although the two curves are close, some interesting differences have to be noticed. The black curve is more regular and is nearly constant until the first bunch TEV starts to fall (around 11 min in figure 7). Then the electrical losses increase gradually while the voltage drops, because the cell operates in a less efficient way.

It can also be noticed that the black curve is generally below the red one and that there is some electrical losses during the relaxation part. This feature is similar to the heat of mixing presented by Thomas and Newman [36] and measured by Chen *et al.* [37] on a LiFePO_4 -graphite cell. The heat of mixing is related to the creation (resp. relaxation) of concentration gradients that consume (resp. generate) some heat. Moreover, the total heat of mixing has to be equal to zero if the cell starts and ends at equilibrium states [36].

Using the data of figure 8, the total energies corresponding to the electrical losses have been calculated for the two approaches and they appeared to be both equal to 44.3 kJ . The characteristics of the heat of mixing are thus respected. The multibunch model provides the perspective of an intrinsic prediction of the heat of mixing because it might be naturally included in its representation of the heterogeneous behavior.

4.5. High stress on the less resistive parts

The 2C discharge simulation demonstrates a heterogeneous stress within the cell. Unsurprisingly, the bunches with the lowest resistances have the higher current rates and the larger SoC drifts (during both discharge and relaxation). These bunches are bound to be more damaged than the others, leading their resistances to increase faster. Consequently, the resistances distribution shape is very likely to evolve and to become more and more left-skewed. This idea at the cell level is consistent with the observation of Schuster *et al.* [27] at the battery-pack level and with the determination of a left-skewed $R_{HF,i}$ distribution for the studied cell in section 6.

To conclude with, the multibunch model is able to reproduce many features of a cell electrical-dynamic, even though its parameters are constant regarding SoC. The simulations were made with a constant current and a constant temperature, making heterogeneity the unique cause for such particular features to appear. The only varying model parameters during the simulation are the $U_{th,i}$ of each bunch, making the strong coupling between the bunches currents and TEV to be a main reason for such a complex electrical-dynamic.

As the relative currents flowing through the bunches depend on the relative $R_{HF,i}$ values, the shape coefficient k has to influence the proposed “heterogeneity signatures”. The next section is dedicated to that point.

5. Influence of the resistance distribution shape

The distribution shape of the $R_{HF,i}$ resistances determines the relative speed of charging or discharging of the bunches. Basically, if the resistances values are more spread, the cell behavior will be more heterogeneous and its macroscopic behavior will be different. This is demonstrated thanks to several simulations of a 2C discharge at 25°C with a RSTD of the high-frequency resistances that

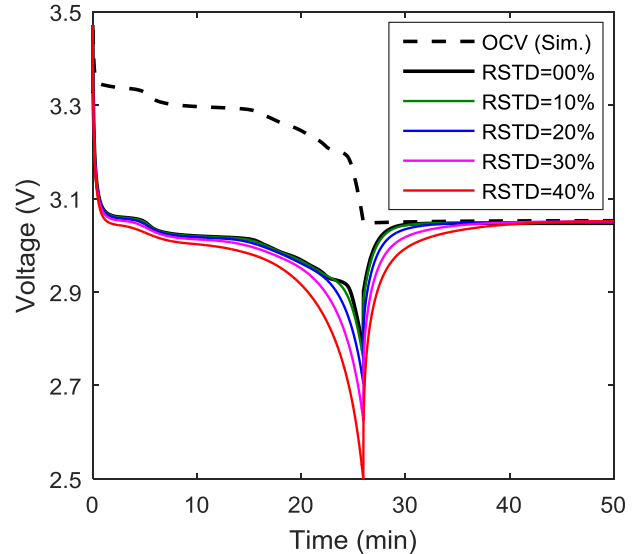


Figure 9: Multibunch model simulations of the 2C discharges of a cell using a Weibull distribution for the $R_{HF,i}$ ($k = 2.5$) and different RSTD values.

varies between 0% and 40%. The distribution is still a Weibull one with a shape parameter of $k = 2.5$ (figure 9). Unsurprisingly, the heterogeneity signatures presented before are more and more pronounced: larger voltage drop, smoother voltage and slower relaxation.

To go further into the study of the distribution-shape impact, several simulations of a cell 2C discharge have been run using different shape coefficients k (figures 10a and 10b). Each distribution has an RSTD of 40% and their equivalent resistances are the same.

A small shape coefficient ($k = 0.7$) leads to a lot of small resistances with close values and a few very high ones (figure 10a). The corresponding voltage response (figure 10b) looks like a homogeneous case as it has a shape close to the OCV, but the relaxation part is the slowest one. This is because most of the bunches are operating at close speeds, apart from a few ones that are sluggish due to their high resistances. During the balancing phase, these very resistive bunches can only exchange a small current with the others, which leads to a slow balancing phase.

The symmetrical distribution case ($k = 3.5$) has a lower and smoother voltage response. The final voltage drop is the quickest. Finally, the right-skewed distribution ($k = 6$) has the same voltage response than the symmetrical case at the beginning, but its final voltage drop is less pronounced and its relaxation is the quickest of all.

Though the RSTD of the $R_{HF,i}$ and their equivalent resistance are the same, all these simulations exhibit very different dynamic responses. Consequently, the internal resistances distribution-shape appear to be an important characteristic of a cell, because it has an impact on its dynamic electrical-behavior, on its performances and eventually on the way it will age (cf. section 4). Moreover, if a given distribution shape leads to a particular dynamic

response, it also means that this distribution can be extracted from measurements. The next and final part is dedicated to the determination of the distribution shape of a commercial cell and to the experimental validation of the multibunch simulation results.

6. Experimental validation

To ensure the quality of the simulation, a model with $n = 100$ bunches has been considered (for more than 100 bunches, no further improvement of the simulation results has been observed). Before comparing its results with the test presented in section 2, the resistance distribution of the studied cell has to be determined. It has been done by solving the optimization problem presented below.

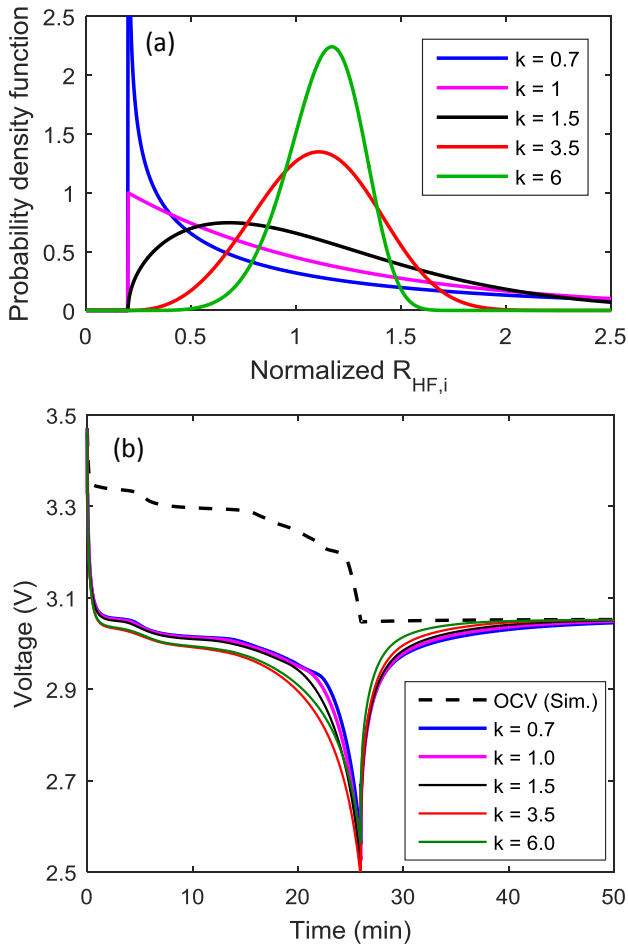


Figure 10: (a) Examples of different Weibull distributions for the $R_{HF,i}$ using the same amplitude ($\lambda = 1$) and localization ($\theta = 0.2$) coefficients but with different shape coefficients k . (b) Simulations of the 2C discharges of a cell with the same equivalent resistances and RSTD for the $R_{HF,i}$ distributions, but different shape coefficients k .

$$\underset{k, \lambda, \theta}{\text{minimize}} \quad f_0(t, k, \lambda, \theta) = \sum (U_{mes}(t) - U_{sim}(t, k, \lambda, \theta))^2$$

$$\text{subject to} \quad k > 0$$

$$\lambda > 0$$

$$R_{HF,i} > 0, \quad i = 1, \dots, n.$$

$$R_{HF,mes}(50\%SoC) = \left(\sum \frac{1}{R_{HF,i}} \right)^{-1}$$

The k , λ and θ parameters of the Weibull distribution (Eq. 3) have been adjusted to minimize the difference between the measured and simulated voltages in the least square sense. As explained in section 3, the equivalent resistance to the $R_{HF,i}$ in parallel has to be equal to $R_{HF,mes}(50\%SoC)$: the high frequency resistance measured for a homogeneous model at 50% SoC.

The optimal distribution found this way has been represented in the figure 11. Its shape coefficient k equals 2 and its RSTD is 35%. This distribution is left-skewed, making it consistent with the feature presented in section 4.5.

The found distribution has been implemented in the multibunch model to simulate the voltage response presented in figure 11a. The simulation results with a homogeneous model (with one bunch), presented in section 2, has also been added to the figure. The heterogeneous model prediction is in accordance with the measurement during the whole 2C discharge. The voltage rise at the end of the charge is well represented but it occurs sooner than the measurement. This must be because the real distribution of the $R_{HF,i}$ is different from its approximation by a Weibull one. The root mean squared error between the multibunch model simulation and the measurements equals 37 mV on the whole test.

The simulation of the relaxation parts is better than with a homogeneous model at the end of the charge (figure 4), but it is still insufficient to match the measurements. This must be due to the current dependency of the electrical parameters which is unclear in open-circuit. Physically, it seems obvious that each bunch parameters should depend on the current flowing through it, but this leads to a parameter-determination problem that is not addressed in this study.

There is a ‘‘bump’’ at the beginning of the 2C discharge that differs from the measured voltage. It appears because the cell is assumed to start in an equilibrate state. Within a real cell, even if the positive electrode is balanced at the end of a charge, there must be some SoC dispersion within the graphite electrode caused by a previous operation (because its open-circuit potential (OCV) is a flat curve, a complete balancing cannot occur). Therefore, the real-cell negative-electrode must start the discharge in a heterogeneous state, thus preventing the first OCV transition due to graphite to be distinguishable on the measurement. As the two electrodes are considered as a whole in the pro-

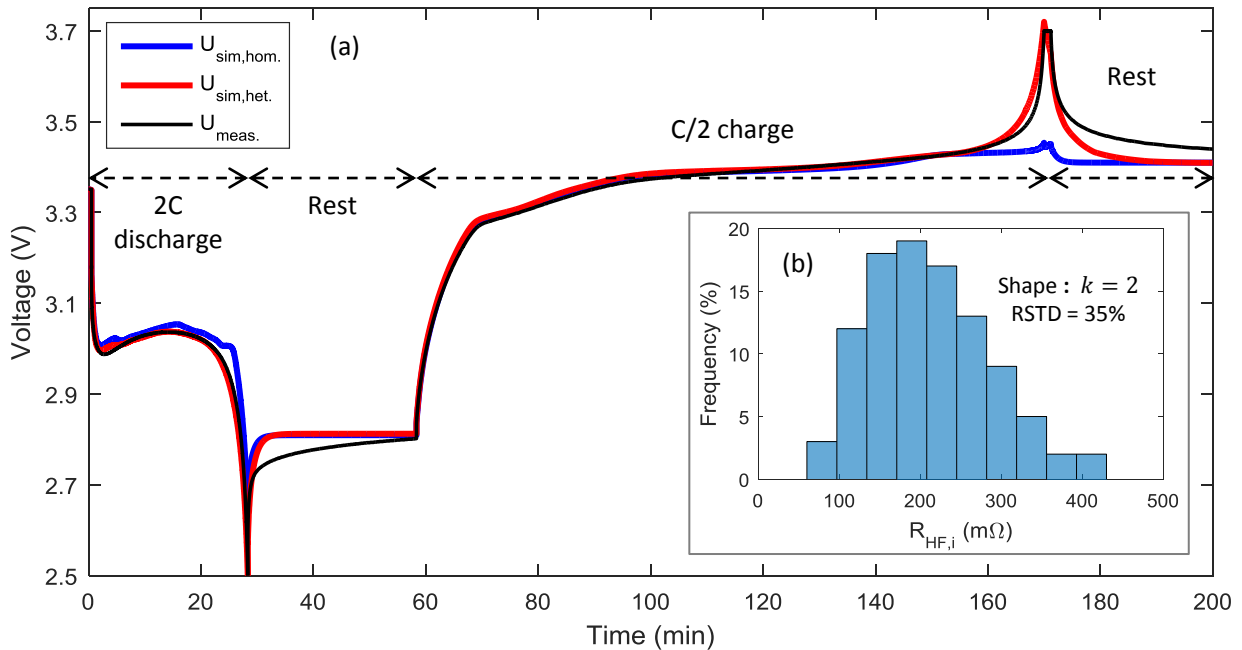


Figure 11: Measurements on the studied cell during the validation test [25]. (a) Measured and simulated cell voltage with the proposed multibunch model, using parameters depending on current and temperature, but constant regarding SoC. The heterogeneous case is simulated with $n = 100$ bunches and the homogeneous case with $n = 1$ bunch. (b) The determined distribution of the studied cell high-frequency resistances $R_{HF,i}$ (shape coefficient $k = 2$ and RSTD = 35%).

posed model, this cannot be represented.

The simulation results confirm the validity of the proposed approach. Though the non-linearities regarding SoC have been removed, the electrical-dynamic is well represented and a realistic internal distribution has been found. The simulation time for the homogeneous case ($n = 1$) was 28.3 s and it has been significantly increased when using $n = 100$ bunches (247 s). In this study, the number of bunches was set to 100 to ensure the quality of the results, but a trade-off between the simulation time and the results accuracy would have to be found if the proposed model was to be used on a regular basis.

7. Conclusion

An ECM has been proposed to model the heterogeneous electrical-behavior of a commercial LiFePO_4 -graphite cell. This “multibunch model” construction is based on a physical approach. Unlike classical homogeneous models, its parameters do not require to be functions of the state of charge to bring accurate results, especially at high current rates and at the ends of charge and discharge. This benefit is bound to significantly reduce the model characterization cost compared to the homogeneous ones, because these SoC non-linearities have classically to be determined for current and temperature values that cover the whole operating range of the battery.

More than 30 working days have been needed to measure the homogeneous Randles model parameters on the

whole SoC range, for five different temperatures (from -5°C to 45°C) and for seven different current values (ranging from 2C in discharge to 1C in charge). By measuring the electrical parameters at only one SoC value, we estimate that the characterization time can be reduced to less than 3 days. We considered that one measure of the electrical parameters requires a mean time of 4 min and that 30 min of relaxation in open-circuit are needed before measuring the next point [25]. We also considered that 4 h are needed for the cell to reach its thermal equilibrium when the characterization temperature is changed.

The multibunch model is constructed by considering a cell as a set of elementary parts with different electrical properties. The parts with close properties have been regrouped in bigger sets called bunches. The latter have been modeled by homogeneous Randles circuits with specific parameters depending on current and temperature. The complete model is obtained by connecting all the bunches models in parallel.

In accordance with recent studies, we chose to use different “high-frequency” resistances for each bunch (this parameter being related to electrolyte, current collectors, charge transfer and contact resistances). The distribution of this parameter has been approximated by a 3-parameter Weibull distribution because its outputs are positive values (if the location parameter θ is positive), which is physically necessary for describing resistances. Moreover, this particular function is more versatile than a classical normal function, because skewness can be described. The diffusion parameter $R_{diff,i}$ and $C_{diff,i}$ have been assumed

to be the same for each bunch.

We proposed an explanation of a cell internal dynamic-behavior *via* the thorough description of the various heterogeneity impacts on a cell electrical-dynamic. It has been demonstrated that the multibunch model is able to represent:

- the disappearance of the OCV shape at high current;
- the decrease of the electrical performances;
- longer relaxation times;
- electrical losses during relaxation in open-circuit;
- higher stress in the less resistive parts of the cell.

The dynamic response of the cell depends significantly on the distribution shape of the internal resistances, making the latter an important feature to be characterized. The high-frequency resistances distribution of a LiFePO_4 -graphite cell has been determined and it appeared to be left-skewed. This result is consistent with the idea of a faster degradation of the cell less-resistive parts during operation.

The proposed model has been experimentally validated. The smooth voltage response of the multibunch model matches the measurements, especially during the 2C discharge and at the end of the charge. The simulation of the relaxation part is better than the prediction of the considered homogeneous model, but it may be further improved by studying the electrical-parameters dependencies to the bunches currents during the balancing.

In the future, it would be interesting to validate the multibunch model on a wider operating range (high current rates, low temperatures, transient operation). To do so, the double layer capacity would have to be considered, as well as several RC cells to properly model the diffusion process during short pulses. Besides, the model response during relaxation parts would have to be improved. The determination of the equivalent internal resistances distribution could be the basis of a non-invasive tool to characterize the quality of a cell or electrode. Besides, its tracking during a battery lifetime would give valuable information on its states of health and function. The proposed model could also be used to rebuild the apparent SoC dependencies of a homogeneous model electrical-parameters, thus significantly reducing the duration of a general cell characterization process.

Acknowledgment

The authors acknowledge the E4V company for its participation to the study and Yves Chabre for its scientific support.

References

- [1] S. Abada, G. Marlair, A. Lecocq, M. Petit, V. Sauvant-Moynot, F. Huet, Safety focused modeling of lithium-ion batteries: A review, *Journal of Power Sources* 306 (2016) 178–192.
- [2] J.-M. Tarascon, Key challenges in future Li-battery research., *Philosophical transactions. Series A, Mathematical, physical, and engineering sciences* 368 (1923) (2010) 3227–41.
- [3] R. Malik, A. Abdellahi, G. Ceder, A Critical Review of the Li Insertion Mechanisms in LiFePO_4 Electrodes, *Journal of the Electrochemical Society* 160 (5) (2013) A3179–A3197.
- [4] S. Miyatake, Y. Susuki, T. Hikiyama, S. Itoh, K. Tanaka, Discharge characteristics of multicell lithium-ion battery with nonuniform cells, *Journal of Power Sources* 241 (2013) 736–743.
- [5] L. Pei, T. Wang, R. Lu, C. Zhu, Development of a voltage relaxation model for rapid open-circuit voltage prediction in lithium-ion batteries, *Journal of Power Sources* 253 (2014) 412–418.
- [6] C. Savard, A. Sari, P. Venet, L. Pietrac, E. Niel, C-3C: A structure for high reliability with minimal redundancy for batteries, in: 2016 IEEE International Conference on Industrial Technology (ICIT), IEEE, 2016, pp. 281–286.
- [7] J. Neubauer, A. Pesaran, The ability of battery second use strategies to impact plug-in electric vehicle prices and serve utility energy storage applications, *Journal of Power Sources* 196 (23) (2011) 10351–10358.
- [8] G. Ouvrard, M. Zerrouki, P. Soudan, B. Lestriez, C. Masquelier, M. Morcrette, S. Hamelet, S. Belin, A. M. Flank, F. Baudelet, Heterogeneous behaviour of the lithium battery composite electrode LiFePO_4 , *Journal of Power Sources* 229 (2013) 16–31.
- [9] P. J. Osswald, S. V. Erhard, J. Wilhelm, H. E. Hoster, A. Jossen, Simulation and Measurement of Local Potentials of Modified Commercial Cylindrical Cells, *Journal of The Electrochemical Society* 162 (10) (2015) A2099–A2105.
- [10] G. Zhang, C. E. Shaffer, C.-Y. Wang, C. D. Rahn, Effects of Non-Uniform Current Distribution on Energy Density of Li-Ion Cells, *Journal of the Electrochemical Society* 160 (11) (2013) A2299–A2305.
- [11] K. Smith, C.-Y. Wang, Power and thermal characterization of a lithium-ion battery pack for hybrid-electric vehicles, *Journal of Power Sources* 160 (1) (2006) 662–673.
- [12] M. Park, X. Zhang, M. Chung, G. B. Less, A. M. Sastry, A review of conduction phenomena in Li-ion batteries, *Journal of Power Sources* 195 (24) (2010) 7904–7929.
- [13] J. Li, Y. Cheng, M. Jia, Y. Tang, Y. Lin, Z. Zhang, Y. Liu, An electrochemical-thermal model based on dynamic responses for lithium iron phosphate battery, *Journal of Power Sources* 255 (2014) 130–143.
- [14] M. Mastali Majdabadi, S. Farhad, M. Farkhondeh, R. A. Fraser, M. Fowler, Simplified electrochemical multi-particle model for LiFePO_4 cathodes in lithium-ion batteries, *Journal of Power Sources* 275 (2015) 633–643.
- [15] D. M. Bernardi, J.-Y. Go, Analysis of pulse and relaxation behavior in lithium-ion batteries, *Journal of Power Sources* 196 (1) (2011) 412–427.
- [16] M. Farkhondeh, M. Safari, M. Pritzker, M. Fowler, T. Han, J. Wang, C. Delacourt, Full-Range Simulation of a Commercial LiFePO_4 Electrode Accounting for Bulk and Surface Effects: A Comparative Analysis, *Journal of the Electrochemical Society* 161 (3) (2014) A201–A212.
- [17] E. Kuhn, C. Forgez, G. Friedrich, Modeling diffusive phenomena using non integer derivatives, *The European Physical Journal Applied Physics* 25 (3) (2004) 183–190.
- [18] L. Mihet-Popa, O. M. F. Camacho, P. B. Norgard, Charging and discharging tests for obtaining an accurate dynamic electro-thermal model of high power lithium-ion pack system for hybrid and EV applications, in: 2013 IEEE Grenoble Conference, no. 10580, IEEE, 2013, pp. 1–6.
- [19] S. Raël, M. Hinaje, Using electrical analogy to describe mass and charge transport in lithium-ion batteries, *Journal of Power Sources* 222 (2013) 112–122.

- [20] J. P. Schmidt, E. Ivers-Tiffée, Pulse-fitting - A novel method for the evaluation of pulse measurements, demonstrated for the low frequency behavior of lithium-ion cells, *Journal of Power Sources* 315 (2016) 316–323.
- [21] N. Watrin, H. Ostermann, B. Blunier, A. Miraoui, Multiphysical Lithium-Based Battery Model for Use in State-of-Charge Determination, *IEEE Transactions on Vehicular Technology* 61 (8) (2012) 3420–3429.
- [22] X. Lin, H. E. Perez, S. Mohan, J. B. Siegel, A. G. Stefanopoulou, Y. Ding, M. P. Castanier, A lumped-parameter electro-thermal model for cylindrical batteries, *Journal of Power Sources* 257 (2014) 1–11.
- [23] J. Illig, Physically based Impedance Modelling of Lithium-ion Cells, Ph.D. thesis (2014).
- [24] M. A. Roscher, D. U. Sauer, Dynamic electric behavior and open-circuit-voltage modeling of LiFePO₄-based lithium ion secondary batteries, *Journal of Power Sources* 196 (1) (2011) 331–336.
- [25] N. Damay, C. Forgez, M.-P. Bichat, G. Friedrich, Thermal modeling of large prismatic LiFePO₄/graphite battery . Coupled thermal and heat generation models for characterization and simulation, *Journal of Power Sources* 283 (2015) 37–45.
- [26] N. Damay, Contribution à la modélisation thermique de packs batteries LiFePO₄ pour véhicules décarbonés, Ph.D. thesis, Université de Technologie de Compiègne (2015).
- [27] S. F. Schuster, M. J. Brand, P. Berg, M. Gleissenberger, A. Jossen, Lithium-ion cell-to-cell variation during battery electric vehicle operation, *Journal of Power Sources* 297 (2015) 242–251.
- [28] D. Shin, M. Poncino, E. Macii, N. Chang, A statistical model of cell-to-cell variation in Li-ion batteries for system-level design, *Proceedings of the International Symposium on Low Power Electronics and Design* (i) (2013) 94–99.
- [29] S. J. Cooper, D. S. Eastwood, J. Gelb, G. Damblanc, D. J. L. Brett, R. S. Bradley, P. J. Withers, P. D. Lee, A. J. Marquis, N. P. Brandon, P. R. Shearing, Image based modelling of microstructural heterogeneity in LiFePO₄ electrodes for Li-ion batteries, *Journal of Power Sources* 247 (2014) 1033–1039.
- [30] M. Fleckenstein, O. Bohlen, M. A. Roscher, B. Bäker, Current density and state of charge inhomogeneities in Li-ion battery cells with LiFePO₄ as cathode material due to temperature gradients, *Journal of Power Sources* 196 (10) (2011) 4769–4778.
- [31] T. Satyavani, B. Ramya Kiran, V. Rajesh Kumar, A. Srinivas Kumar, S. Naidu, Effect of particle size on dc conductivity, activation energy and diffusion coefficient of lithium iron phosphate in Li-ion cells, *Engineering Science and Technology, an International Journal* 19 (1) (2016) 40–44.
- [32] P. Mauracher, E. Karden, Dynamic modelling of lead/acid batteries using impedance spectroscopy for parameter identification, *Journal of Power Sources* 67 (1-2) (1997) 69–84.
- [33] G. Zhang, C. E. Shaffer, C.-Y. Wang, C. D. Rahn, In-Situ Measurement of Current Distribution in a Li-Ion Cell, *Journal of the Electrochemical Society* 160 (4) (2013) A610–A615.
- [34] J. Illig, M. Ender, A. Weber, E. Ivers-Tiffée, Modeling graphite anodes with serial and transmission line models, *Journal of Power Sources* 282 (2015) 335–347.
- [35] C. Heubner, M. Schneider, A. Michaelis, Investigation of charge transfer kinetics of Li-Intercalation in LiFePO₄, *Journal of Power Sources* 288 (2015) 115–120.
- [36] K. E. Thomas, J. Newman, Heats of mixing and of entropy in porous insertion electrodes, *Journal of Power Sources* 119-121 (2003) 844–849.
- [37] K. Chen, G. Unsworth, X. Li, Measurements of heat generation in prismatic Li-ion batteries, *Journal of Power Sources* 261 (2014) 28–37.